World Journal of Innovation and Modern Technology, Vol. 8, Issue 5, (May)
ISSN 2682-5910 2025

DOI: 10.53469/wjimt.2025.08(05).21

Research on the Strategy of Pd Atomic-Level Dispersion Driven by Multi-Metal Synergistic Effects and Its Catalytic Oxidation Performance

Zhou Fan

College of Materials Science and Engineering, Xi'an Shiyou University, Xi'an 710065, Shaanxi, China

Abstract: ***In this study, Pd-Ce@Al_2O_3 and Pd-Ce-Cu(1:1)@Al_2O_3 binary and ternary metal catalysts were successfully prepared by the non-polar solvent displacement method, and single-metal Pd@Al_2O_3 was simultaneously prepared as a comparison system. The effects of the introduction of co-catalysts such as Ce and Cu on the dispersion and particle size distribution of Pd noble metal were systematically investigated by high-resolution transmission electron microscopy (HR-TEM) combined with energy dispersive X-ray spectroscopy (EDS). It was found that the introduction of CeO_2 significantly improved the dispersion of Pd species through the strong metal-support interaction (SMSI effect), and the co-doping of Cu further optimized the electronic structure of the active sites, resulting in the ternary catalyst showing the best low-temperature catalytic performance. This study provides a new component regulation strategy and theoretical basis for the design of efficient Pd noble metal catalysts.***

Keywords: Precious metal; Catalyst dispersion; Metal doping; Hydrogen catalytic oxidation.

1. INTRODUCTION

Among the numerous hydrogen catalytic oxidation catalysts, the precious metal Pd is regarded as a key material in the field of low-temperature deoxidation due to its excellent redox activity and stability [1]. However, traditional Pd-based catalysts generally have problems such as poor dispersion of precious metals [2], low atomic utilization rate [3], and easy sintering [4], which seriously restrict their large-scale industrial application. Against this background, the development of PD-based catalysts with high dispersion and high activity has become a cutting-edge topic in the design of catalytic materials [5]. Although the atomic-level dispersion strategy of precious metals has significant advantages, its practical application still faces multiple challenges: insufficient stability of active sites, Pd nanoparticles are prone to deactivation due to sintering or oxidation at low loading, especially with obvious performance attenuation in high-temperature or high-humidity environments [6]. However, most existing studies are limited to a single carrier type and lack systematic optimization. This chapter proposes the "multi-component structure regulation" strategy to construct efficient Pd-based catalysts through the following approaches. Firstly, Al_2O_3 carriers with high specific surface area are selected. Then, CeO_2 cocatalysts are introduced as the primary component. By taking advantage of their strong oxygen storage/release capacity, the Pd^0/Pd^{2+} redox cycle is promoted and particle agglomeration is inhibited [7]. The transition metal Cu was introduced to form the alloyed secondary components and create the Pd-Cu alloy interface [8]. The center position of the D-band of Pd was regulated through the electron transfer effect (Cu→Pd) [9] to optimize the adsorption energy and reaction path of H_2. The optimization of this structure not only enhances the catalytic efficiency of the catalyst under low loading but also makes its application in complex reaction systems possible.

2. EXPERIMENTAL SECTION

2.1 Preparation of Catalysts

Add the n-octanol solution to the alumina balls and conduct ultrasonic treatment for 30 minutes to ensure that n-octanol fully penetrates into the interior of the alumina balls. The excess hydrophobic solvent on the surface of the alumina balls is removed through filtration operation. Prepare 60 mL of 3.0 mol/L cerium nitrate solution. Dissolve copper nitrate with (Ce/Cu = 0.1) into the above-mentioned cerium nitrate solution and mix evenly. The treated alumina carrier was added to the above mixed solution and over-impregnated for 5 minutes, and then the impregnated alumina balls were filtered out. The impregnated alumina balls were dried at 80℃ for 10 h and then calcined at 500℃ for 4 h to obtain catalyst carriers, which were named Ce@Al_2O_3 and Ce-Cu(1:1)@Al_2O_3. 100

mL of 0.125 g-Pd/L chloropalladium acid solution was prepared and the pH of the solution was adjusted to 3. The different eggshell-shaped carriers prepared above were added to the diluted chloropalladium acid solution and the redox reaction was carried out at 50°C for 5 hours. After the reaction was completed, the catalysts were separated by filtration and dried at 80°C for 13 h to obtain Pd@Al_2O_3, Pd-Ce@Al_2O_3, Pd-Ce-Cu(1:1)@Al_2O_3 catalysts.

2.2 Catalyst Characterization Methods

In this paper, transmission electron microscope (model JEM-2100 F, JEOL Ltd., Japan) is used to analyze the low-resolution morphology, high-resolution morphology (HRTEM) and energy dispersive X-ray spectroscopy (EDS) mapping of the samples, with a constant acceleration voltage of 200 kV.

3. RESULTS AND DISCUSSION

Figure 1 (a-f) shows HRTEM of Pd@Al_2O_3 catalyst and TEM-mapping of Pd, O and Al elements. It can be seen from the HAADF-STEM image in Figure 1(a) that porous Al_2O_3, as the carrier material, has good porosity and specific surface area, providing dispersed support for Pd nanoparticles. Figure 1(b-c) shows the distribution of O and Al in Pd@Al_2O_3 catalyst. The Al signal is mainly concentrated in the substrate region, indicating that Al_2O_3 is the main carrier material. The distribution of O is also relatively uniform, covering the entire catalyst region, indicating abundant oxygen species in the catalyst. The TEM-mapping image in Figure 1(d) shows the distribution of Pd, representing the signal strength of Pd. The brighter the area, the higher the concentration of Pd. Pd is dispersed on the surface of Al_2O_3 in the form of nanoclusters, and it can be clearly seen that partial agglomeration of Pd has occurred. Figure 1(e-f) shows that Pd nanoparticles are uniformly distributed on the Al_2O_3 substrate. The size of the Pd particles is relatively small, approximately 10nm, and partial agglomeration has occurred, indicating that the dispersion of the traditional direct loading of Pd on Al_2O_3 is poor.

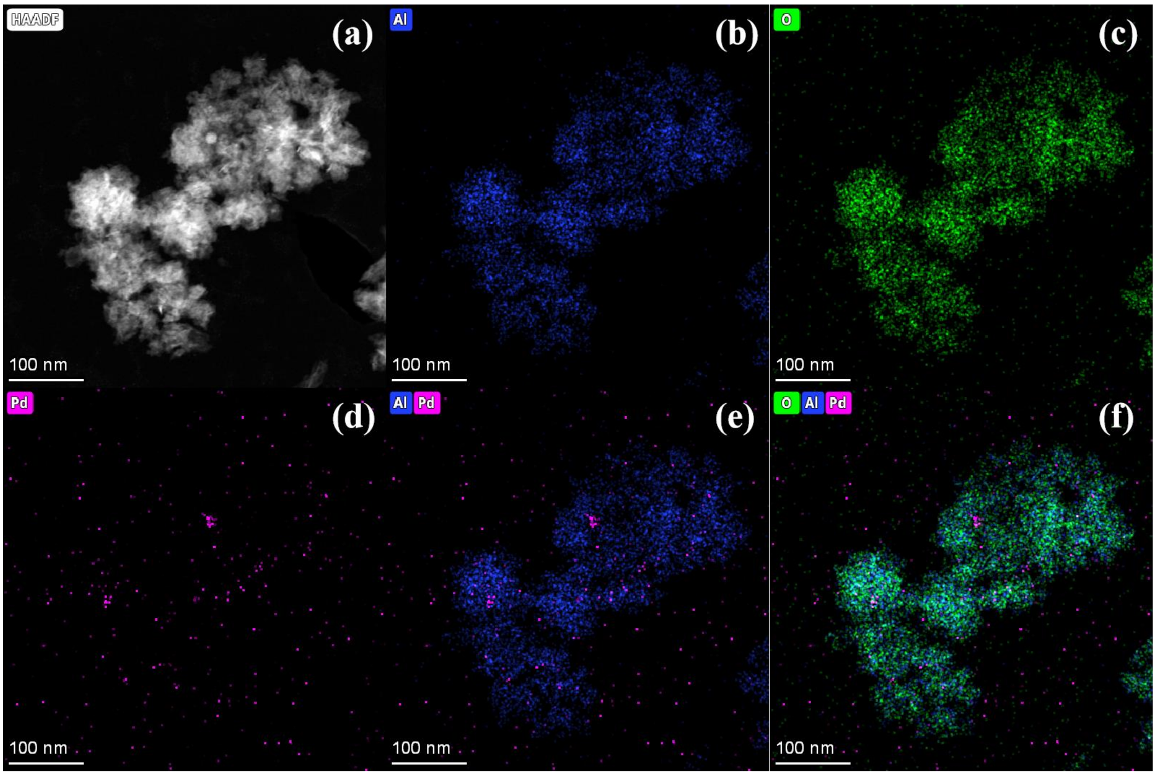

Figure 1: HRTEM of Pd@Al_2O_3 catalyst and mapping of Pd, O and Al elements

Figure 2 shows HRTEM of Pd-Ce@Al_2O_3 catalyst and TEM-mapping of Pd, Ce, O and Al elements. It can be seen from the HAADF-STEM image in Figure 2(a) that the carrier modified by CeOx still maintains the high-porosity structure of Al_2O_3. Figure 2(b-e) shows the TEM-mapping images of Al, O, Ce and Pd elements respectively. It can be seen from the figures that Ce is uniformly covered on the surface of Al_2O_3 in the form of nanoparticles or oxides. The Pd particles are small in size (speculated to be <2 nm) and evenly dispersed, indicating that the optimized preparation process effectively avoids particle agglomeration. The high dispersion can significantly increase the density of active sites and enhance catalytic activity. Figure 2(f) shows the superimposed distribution of Pd, Ce and Al_2O_3. It can be seen that Pd and CeOx are in contact with each other, which also proves the reduction loading process of Pd, indicating that the addition of Ce components has improved the dispersion of the precious metal Pd.

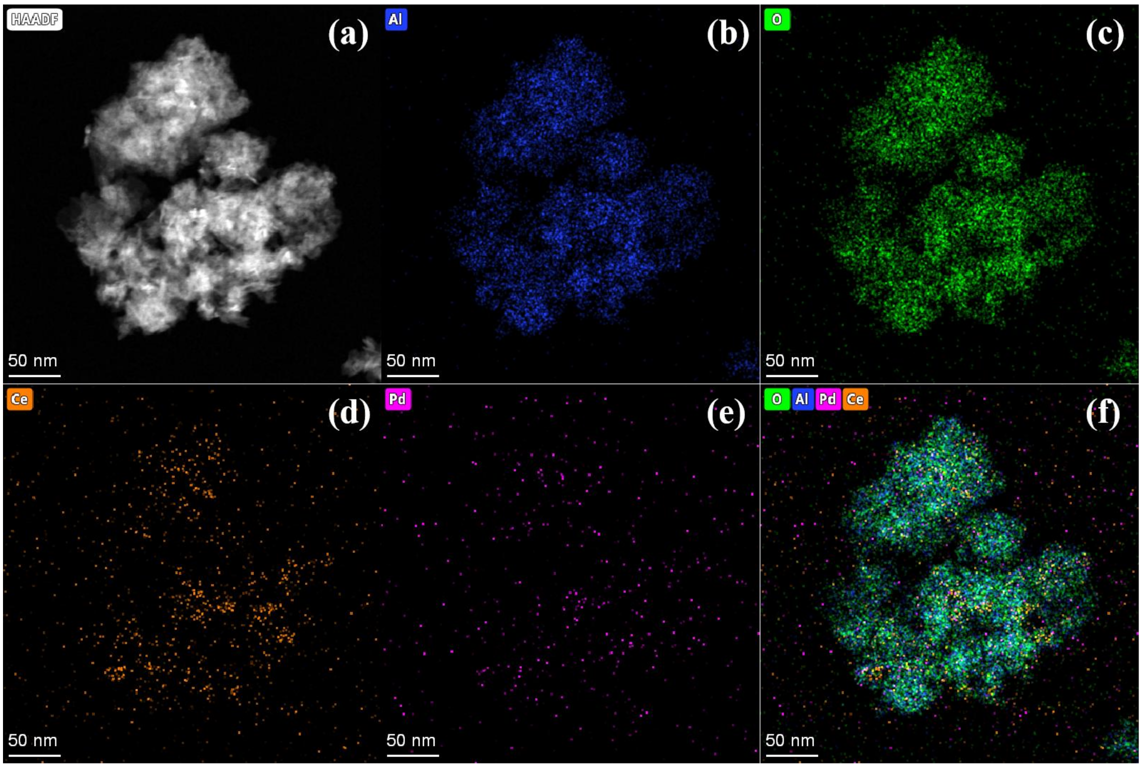

Figure 2: HRTEM of Pd-Ce@Al_2O_3 catalyst and mapping of Pd, Ce, O and Al elements

Figure 3 shows the HRTEM of the PD-CE-Cu(1:1)@Al_2O_3 catalyst and the TEM-mapping diagrams of Pd, Ce, Cu and Al elements. As can be seen from the HAADF-STEM image in Figure 3(a), the catalyst is similar to Pd-Ce@Al_2O_3 and retains the morphology of Al_2O_3. Figure 3(b-e) shows the TEM-mapping images of Al, Cu, Ce and Pd elements respectively. It can be seen from the figures that the Al element presents a relatively uniform distribution in the catalyst, and the signal intensity changes relatively gently throughout the observation area. It covers the entire catalyst area, which may be related to the structure and surface properties of the Al_2O_3 carrier. However, the Cu and Ce elements are uniformly distributed, indicating that CeOx is highly dispersed on the surface of Al_2O_3. In the area with a higher copper content, Ce, Cu, and Pd are all uniformly distributed, indicating that there is an interaction between CeOx and CuOx. The distribution of Pd elements has a consistent relationship with that of Cu. It indicates that the loading process of Pd forms a PdCu alloy structure, and Pd is atomically dispersed on the Al_2O_3 carrier. Figure 3(f) shows the superposition distribution of Al, Pd, Ce, Cu, O, and Al. Ce can stabilize Pd particles through anchoring, similar to the mechanism in Pd-Ce@Al_2O_3. Cu may form a ternary interface with Pd and Ce in the form of oxides or alloys. This Pd-Cu-Ce composite structure may enhance the electron interaction. It is indicated that the addition of Ce and Cu components has further improved the dispersibility of the precious metal Pd.

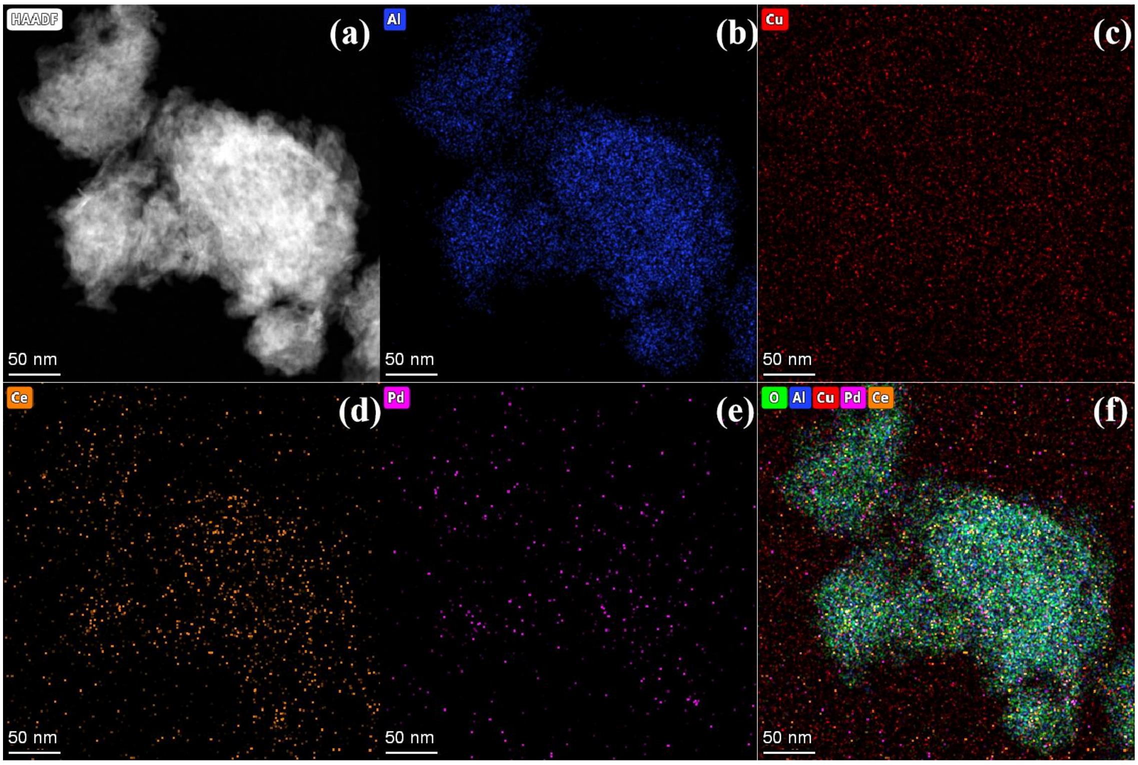

Figure 3: HRTEM of Pd-Ce-Cu(1:1)@Al_2O_3 catalyst and mapping diagrams of Pd, Ce, Cu, O and Al elements

In the field of hydrogen-catalyzed oxidation, the Pd@Al_2O_3 system is widely used, but the low temperature activity of its single-metal catalyst has always been the focus of research. Figure 4 shows the catalytic activities of Pd-based catalysts with different components. Under the experimental conditions of a total flow rate of 400 mL/min (including 290 mL/min for 5%H_2/N_2 and 110 mL/min for 0.2%O_2/N_2) and a total pressure of 0.1 MPa, Through the analysis and comparison of Figure 4, it is found that in the low-temperature section (<150℃) of the ternary Pd-Ce-Cu(1:1)@Al_2O_3 catalyst, It has higher catalytic activity. This phenomenon can be attributed to the electronic synergy between Cu^{2+} and Ce^{3+}. This atomic-level interaction effectively enhances the activation ability of reactive oxygen species on the catalyst surface, thereby improving the catalytic activity. According to the experimental results, the catalytic activity patterns of each catalyst are as follows: Pd-Ce-Cu(1:1)@Al_2O_3 > Pd-Ce@Al_2O_3> Pd@Al_2O_3.

In this study, the introduction of the transition metal Ce demonstrated a unique and crucial electronic regulatory role. The Ce species form a Pd-Ce-O interface structure with Pd, and this structure significantly alters the center position of the d band of the precious metal Pd. The rearrangement effect of electrons not only enhances the dispersion degree of Pd nanoparticles on the γ-Al_2O_3 carrier, but more importantly, optimizes the dissociation adsorption energy barrier of H_2 molecules at the active site. The introduction of metallic Cu might be due to the different redox potentials between Ce^{4+}/Ce^{3+} and $Cu^{2+}$and Cu^{+}, thereby generating a large amount of Cu^{+}, which effectively increases the ability of the catalyst to activate oxygen. The above-mentioned research indicates that by precisely designing multi-component catalysts, more highly active sites can be exposed compared to traditional single-metal catalysts, improving the dispersion of precious metal atoms and enhancing the catalytic activity of the catalyst.

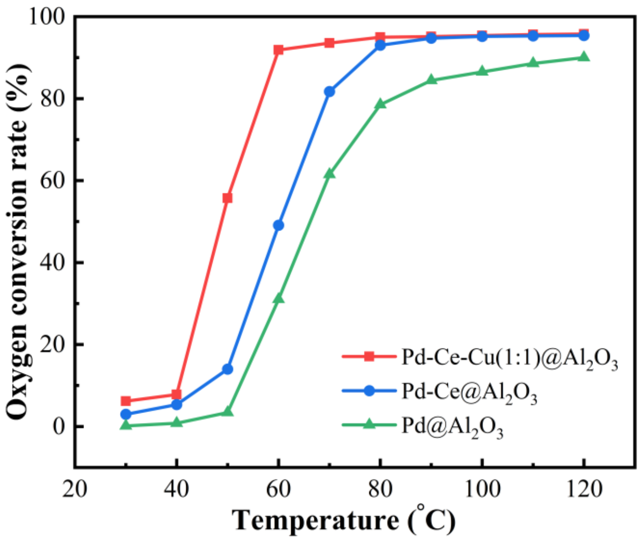

Figure 4: The influence of different co-active components on the catalytic activity of Pd-based catalysts

4. CONCLUSION

The characterization results of transmission electron microscopy (TEM) show that the three elements Pd, Ce and Cu are uniformly dispersed on the surface of the catalyst, and the internal carrier maintains a porous skeleton structure. This structure effectively shortens the diffusion path of the reactants. In the hydrogen catalytic oxidation reaction, the Pd-Ce-Cu(1:1) @Al_2O_3 catalyst demonstrated optimal catalytic performance, with T_{50} as low as 50℃and T_{90} as low as 60℃, showing a significant performance improvement compared to the Pd@Al_2O_3 catalyst (T_{90} as low as 54℃). The significant improvement in this performance can be attributed to the synergistic effect of Ce and Cu. This synergistic effect not only significantly enhances the catalyst's activation ability for oxygen but also improves the dispersion of Pd, thereby enhancing the overall catalytic activity. Specifically, the addition of the Ce component effectively enhanced the dispersion of Pd atoms. The combined addition of the Ce and Cu components further improved the dispersion of Pd atoms and the atomic utilization rate of Pd, thereby significantly enhancing the catalytic activity of the catalyst. It provides an important basis for the correlation between structure and performance for the design and optimization of efficient hydrogen catalytic oxidation catalysts.

REFERENCES

[1] Seo M-G, Kim H J, Han S S, et al. Effect of shell thickness of Pd core-porous SiO_2 shell catalysts on direct synthesis of H_2O_2 from H_2 and O_2 [J]. Journal of Molecular Catalysis A: Chemical, 2017, 426: 238-243.
[2] Wang C, An C, Qin C, et al. Noble Metal-Based Catalysts with Core-Shell Structure for Oxygen Reduction Reaction: Progress and Prospective [J]. Nanomaterials, 2022, 12(14): 2480-2494.
[3] Fiorenza R. Bimetallic Catalysts for Volatile Organic Compound Oxidation [J]. Catalysts, 2020, 10(6): 661-687.
[4] Das S, Pérez-Ramírez J, Gong J, et al. Core–shell structured catalysts for thermocatalytic, photocatalytic, and electrocatalytic conversion of CO_2 [J]. Chemical Society Reviews, 2020, 49(10): 2937-3004.
[5] Shen J, Hayes R E, Wu X, et al. 100° Temperature Reduction of Wet Methane Combustion: Highly Active Pd–Ni/Al_2O_3 Catalyst versus Pd/$NiAl_2O_4$ [J]. ACS Catalysis, 2015, 5(5): 2916-2920.
[6] Wang J, Yu H, Ma Z, et al. Enhanced Stability of CaO and/or La_2O_3 Promoted Pd/Al_2O_3 Egg-Shell Catalysts in Partial Oxidation of Methane to Syngas [J]. Molecules, 2013, 18(7): 8289-8297.
[7] Xu R, Du L, Adekoya D, et al. Well-Defined Nanostructures for Electrochemical Energy Conversion and Storage [J]. Advanced Energy Materials, 2021, 11(15): 2001537.
[8] Mo F, Zhou Q, Li C, et al. Diatomic catalysts for Fenton and Fenton-like reactions: a promising platform for designing/regulating reaction pathways [J]. Chemical Science, 2023, 14(29): 7818-7827.
[9] Kim J, Tahmasebi A, Lee J M, et al. Low-temperature catalytic hydrogen combustion over Pd-Cu/Al_2O_3: Catalyst optimization and rate law determination [J]. Korean Journal of Chemical Engineering, 2023, 40(6): 1317-1330.